Three-Dimensional Models of Non-NMDA Glutamate Receptors

Michael J. Sutcliffe,* Z. Galen Wo,‡ and Robert E. Oswald‡
*Department of Chemistry, University of Leicester, Leicester LE1 7RH England, and ‡Department of Pharmacology, College of Veterinary Medicine, Cornell University, Ithaca, New York 14853 USA

ABSTRACT Structural models have been produced for three types of non-NMDA ionotropic glutamate receptors: an AMPA receptor, GluR1; a kainate receptor, GluR6; and a low-molecular-weight kainate receptor from goldfish, GFKARα. Modeling was restricted to the domains of the proteins that bind the neurotransmitter glutamate and that form the ion channel. Model building combined homology modeling, distance geometry, molecular mechanics, interactive modeling, and known constraints. The models indicate new potential interactions in the extracellular domain between protein and agonists, and suggest that the transition from the "closed" to the "open" state involves the movement of a conserved positive residue away from, and two conserved negative residues into, the extracellular entrance to the pore upon agonist binding. As a first approximation, the ion channel domain was modeled with a structure comprising a central antiparallel β-barrel that partially crosses the membrane, and against which two α-helices from each subunit are packed; a third α-helix packs against these two helices in each subunit. Much, but not all, of the available data were consistent with this structure. Modifying the β-barrel to a loop-like topology produced a model consistent with available data.

INTRODUCTION

Glutamate-gated cation channels (also known as ionotropic glutamate receptors; iGluRs) are the primary excitatory neurotransmitter receptors in vertebrate brain and play a role in a wide variety of normal (e.g., learning and memory) and pathological (e.g., epilepsy) processes. These receptors exist in a number of different subtypes that are grouped according to their selective agonists (Monaghan et al., 1989). These include the AMPA receptor subunits (GluR1 to 4), the kainate receptor subunits (GluR5 to 7 and KA1 to 2), and the NMDA receptor subunits (NMDAR1 and NMDAR2A to D; Hollmann and Heinemann, 1994; Nakanishi, 1992; Wisden and Seeburg, 1993). In addition, kainate receptors of lower molecular mass (40–50 kDa, also known as kainate binding proteins) have been cloned from nonmammalian vertebrates (e.g., frog, Wada et al., 1989; chick, Gregor et al., 1989; and goldfish, Wo and Oswald, 1994) and exhibit considerable sequence homologies with the C-terminal portions of the 100 kDa mammalian brain AMPA/kainate receptors.

Originally, the glutamate-gated ion channels were assumed to be structurally similar to other ligand-gated ion channels, such as the nicotinic acetylcholine receptor and the $GABA_A$ receptors (Nakanishi and Masu, 1994). Based on the hydropathy profile and this presumed homology, iGluRs were thought to consist of four transmembrane domains (see Fig. 1 *A*), with both the N- and C-termini located extracellularly and with a large cytoplasmic loop between the third (TMIII) and fourth (TMIV) transmembrane domains. However, we demonstrated recently that the transmembrane topology of lower-molecular-mass kainate receptors differs significantly from other ligand-gated ion channels and consists of three transmembrane domains (Wo and Oswald, 1994, 1995b). This was subsequently confirmed by Hollmann et al. (1994) on GluR1 and Bennett and Dingledine (1995) on GluR3. The revised view of glutamate receptor topology is shown schematically in Fig. 1 *B*. Two major features of this model are immediately apparent: 1) the extracellular portion consists of the N-terminal region of the protein before the first transmembrane segment and the loop between what has been previously referred to as the third and fourth transmembrane domains, and 2) the second transmembrane segment does not traverse the membrane but, based on its role in ion conduction, is probably inserted into the ion-conducting pathway in a manner similar to the P-segment in K^+ and cyclic nucleotide-gated channels. The extracellular regions of the protein have been shown to be homologous to bacterial periplasmic amino acid binding proteins (Nakanishi et al., 1990; O'Hara et al., 1993). The new model of glutamate receptor structure (Hollmann et al., 1994; Stern-Bach et al., 1994; Wo and Oswald, 1994, 1995b,c) places all of the regions homologous to the bacterial proteins on the extracellular side of the membrane and immediately suggests the possibility that these regions of the receptor evolved from the bacterial amino acid binding proteins (Wo and Oswald, 1995c). The channel portion can be thought of as similar to the ion-conducting portion of a K^+ channel rotated 180° with respect to the plasma membrane. In fact, the putative second transmembrane region of glutamate receptors has significant sequence homology to the corresponding region of voltage-gated K^+ channels (Wo and Oswald, 1995c; Wood et al., 1995). Thus, glutamate receptors seem to be modular proteins constructed from either one (50 kDa nonmammalian vertebrate kainate receptors) or two (all other glutamate receptors) domains evolved from bacterial binding proteins. A relatively hydrophobic

Received for publication 5 July 1995 and in final form 3 January 1996.
Address reprint requests to Dr. Robert E. Oswald, Department of Pharmacology, College of Veterinary Medicine, Cornell University, Ithaca, NY 14853. Tel.: 607-253-3877; Fax: 607-253-3659; E-mail: reo1@cornell.edu.

0006-3495/96/04/1575/15 $2.00

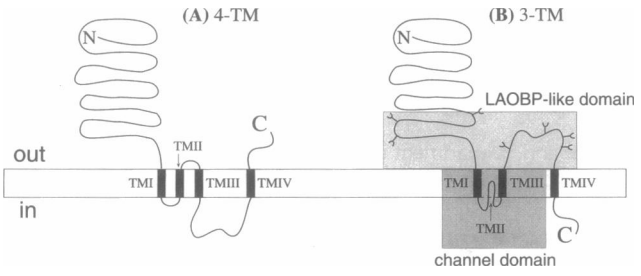

FIGURE 1 (*A*) 4-TM model. Schematic representation of the original model for the transmembrane topology of iGluRs, which was based on presumed homology with other ligand-gated ion channels and hydropathy plots. (*B*) 3-TM model. The current model of the transmembrane topology of iGluRs. The domains that are considered here (the LAOBP-like domain and the channel domain) are highlighted with gray shading. The position of *N*-glycosylation sites in various subunits of non-NMDA receptors is indicated by Y.

voltage-gated K^+ channel-like pore is inserted into one of these domains (Wo and Oswald, 1995c). Finally, the C-terminal portion of these receptors seems to be a regulatory module of unknown origin. The evidence supporting the notion of a modular design for these receptors has been described in detail elsewhere (Wo and Oswald, 1995c).

The first detailed homology modeling study of glutamate receptors (O'Hara et al., 1993) concentrated on a class of glutamate receptors linked to second messengers (known as metabotropic glutamate receptors). Like the glutamate-gated ion channels, these receptors have homologies to bacterial amino acid binding proteins. These techniques were subsequently used to produce a preliminary model of one of the modules of the glutamate-gated ion channels (Stern-Bach et al., 1994). This model was based on the homology between glutamate receptors and bacterial binding proteins, which was supported by site-directed mutagenesis (Kuryatov et al., 1994) and studies of chimeric receptors (Stern-Bach et al., 1994). We describe here detailed models of two of the four modules of glutamate-gated ion channels: 1) the glutamate-binding module with sequence homology to the lysine/arginine/ornithine binding (LAOBP) and glutamine binding (QBP) proteins; and 2) the channel module with homologies to voltage-gated K^+ channels. The N-terminal extracellular region of 100 kDa glutamate receptors is homologous in sequence to several other bacterial proteins, in particular the leucine, isoleucine, valine-binding protein (LIVBP; O'Hara et al., 1993). We did not include this domain in the model because 1) high-affinity agonist binding can be achieved without this domain, as in the case of the 50 kDa kainate receptors (Wada et al., 1989); 2) this region is poorly conserved among glutamate receptors (Hollmann and Heinemann, 1994); and 3) replacement of the GluR1 LIVBP domain with the corresponding domain from NMDA receptors had no functional consequence (Stern-Bach et al., 1994). Three prototypic non-NMDA glutamate receptors were chosen for modeling: 1) GluR1 (also known as GluRA; Hollmann et al., 1989; Keinänen et al., 1990), a 100 kDa AMPA receptor subunit from rat brain; 2) GluR6 (Egebjerg et al., 1991), a 100 kDa kainate receptor subunit; and 3) GFKARα (Wo and Oswald, 1994), a 50 kDa kainate receptor subunit. These representative subtypes of non-NMDA glutamate receptor subunits share more than 40% overall sequence identity. The models are consistent with 1) the known positions of glycosylation in native subunits, 2) the disulfide bonding pattern in the LAOBP/QBP-like domain, and 3) the site-directed mutagenesis and chimeric receptor studies of both the LAOBP/QBP-like domain and the channel domain. The spatial relationship between the glutamate-binding domain and the channel domain coupled with the hinge motion known to occur upon binding amino acids in bacterial binding proteins immediately suggests a possible mechanism for channel opening. The models presented here should be viewed strictly as testable hypotheses, based as much as possible on currently available data, rather than as definitive three-dimensional structures of these proteins.

MATERIALS AND METHODS

Homology modeling

The amino acid sequences of 14 members of the glutamate receptor superfamily were multiply aligned with three bacterial periplasmic amino acid binding proteins for the LAOBP-like domain (Fig. 2), using both Multal (Taylor, 1988) within the program CAMELEON (Oxford Molecular, Oxford, England) and Clustal V (Higgins et al., 1992). The consensus alignment was subject to the constraints that 1) wherever possible, no insertion or deletion occurred within the crystallographically determined secondary structural elements of the bacterial periplasmic amino acid-binding proteins LAOBP (holo and apo forms; Brookhaven Protein Data Bank (Abola et al., 1987; Bernstein et al., 1977) accession numbers 1lst and 2lao (Oh et al., 1993), respectively) and histidine-binding protein (HBP, holo form; 1hsl, Yao et al., 1994), as defined in the respective "extended secondary structure" entries in the IDITIS database of protein structures (Oxford Molecular); 2) the known *N*-glycosylation sites (Hollmann et al., 1994; Roche et al., 1994; Taverna et al., 1994; Wo and Oswald, 1994, 1995a) corresponded to surface positions; and 3) those residues thought to be involved in ligand binding (Kuryatov et al., 1994; Li et al., 1995; Uchino et al., 1992) were positioned in the ligand-binding site.

This sequence alignment was used as the basis for homology modeling, in conjunction with the program COMPOSER (Blundell et al., 1988). A total of six models of the LAOBP domain were produced: the apo and holo forms of GFKARα, GluR1, and GluR6. The apo models were based on LAOBP (2lao), and the holo models on LAOBP (1lst) and HBP (1hsl). The parts of the structures defined as structurally conserved ("framework") regions, and therefore used as the basis of the model, are shown in Fig. 2. In all cases, the "loop" regions joining consecutive framework regions were found by scanning a database of protein structures (within COMPOSER) for a fragment of the correct length and end point geometry for the "loop" in question. The structures were subsequently refined by simulated annealing, followed by energy minimization, using XPLOR (Brunger, 1992). For the initial stage of the simulated annealing, the disulfide bond was formed by fixing the positions of all the atoms except those in the two loops containing the two half-cystines (corresponding to C732 and C787 in GluR1), adding a distance restraint to form this disulfide bond, and using a low repulsive nonbonded force constant (0.01 kcal/mol/Å^4). During the next stage, keeping the same atomic positions fixed, the disulfide bond was added explicitly and the repulsive nonbonded force constant gradually increased from 0.01 kcal/mol/Å^4 to 10.0 kcal/mol/Å^4. The temperature was then slowly reduced from 1000 K to 300 K, and the energy of the structure was minimized. A subsequent energy minimization was performed, with

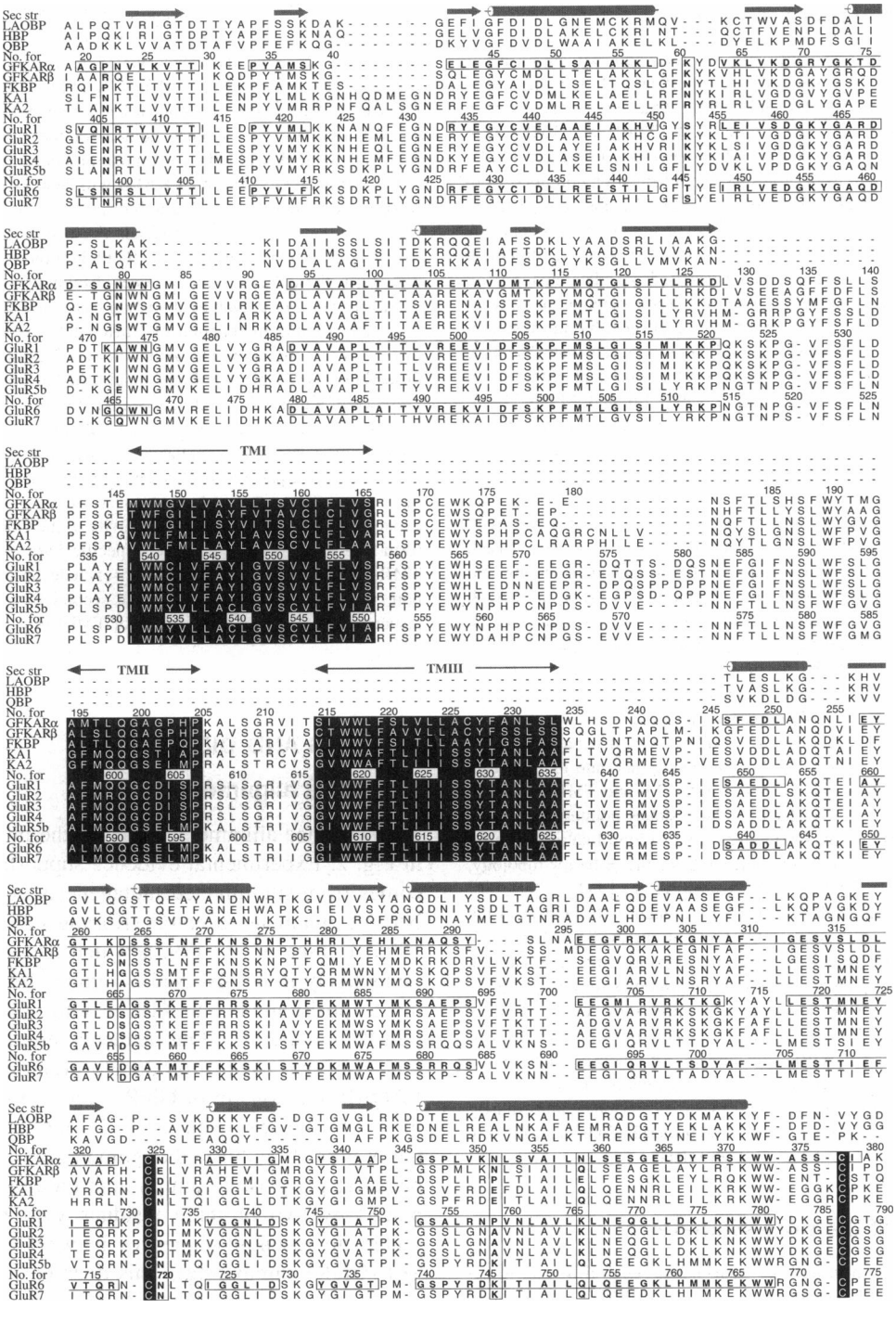

FIGURE 2 Sequence alignment of bacterial periplasmic binding proteins and ionotropic glutamate receptors. The region shown includes the bacterial periplasmic protein-like domain of the glutamate receptors, together with the "inserted" voltage-gated K^+ channel-like domain. The amino acid numbering (starting at the beginning of the signal sequence) for GFKARα, GluR1, and GluR6 is shown, together with the consensus of the secondary structure observed in the structures of bacterial periplasmic amino acid binding proteins; the "framework" regions used in the modeling for GFKARα, GluR1, and GluR6, respectively (*horizontal boxes*); the positions of TMI, TMII, and TMIII in the glutamate receptors (*black background*); glycosylation sites (*vertical boxes across all iGluR sequences*); and the two half-cystines forming the disulfide bond (*black background*). The vertical white line in TMII, immediately after S606 in GluR1, denotes the C-terminal extremity of TMII in the β-barrel topology. This figure was generated using ALSCRIPT (Barton, 1993).

all the atoms free to move, for a further 300 steps, gradually increasing the repulsive nonbonded force constant from 0.1 kcal/mol/Å^4 to 10.0 kcal/mol/Å^4, before minimizing for a further 200 steps using the full nonbonded potential described by the CHARMM 22 forcefield (Mackerell et al., 1992). All calculations were performed in vacuo. The models were inspected visually by using the interactive molecular graphics programs InsightII (Biosym, San Diego, CA) and QUANTA (Molecular Simulations, Boston, MA).

Modeling transmembrane regions

The number of transmembrane segments and their approximate locations have been determined experimentally (Bennett and Dingledine, 1995; Hollmann et al., 1994; Wo and Oswald, 1994, 1995a,b,c). The positions in the sequence of the transmembrane regions TMI, TMIII, and TMIV were determined using the programs MEMSAT (Jones et al., 1994) and TMAP (Person and Argos, 1994). Both programs use information compiled from known transmembrane helical segments to predict the positions of transmembrane helices, if they are likely to exist, in an amino acid sequence. A consensus of the transmembrane regions 1) across the sequence alignment and 2) between the two different programs was used. The detailed topology of the P-segment (TMII) in iGluRs is unknown. The P-segment of voltage-gated K^+ channels was originally modeled as a β-sheet hairpin insertion (Durell and Guy, 1992); however, a revised model suggests that it is not in a β-sheet conformation (Guy and Durell, 1994), consistent with several recent experimental reports (Kurz et al., 1995; Lu and Miller, 1995; Pascual et al., 1995). The P-segment of a potassium channel of the inward rectifier gene family has also been modeled as an inserted β-barrel (Stanfield et al., 1994). For simplicity, the P-segment was initially modeled as an antiparallel β-barrel using XPLOR (Brunger, 1992). As described below, many but not all of the currently available data are consistent with this topology. Twenty models were generated for the P-segment of each channel using distance geometry, followed by simulated annealing and energy minimization. The models were restrained to be symmetrical, appropriate hydrogen bond and dihedral angle restraints were applied to the β-strands (see Fig. 5 *A*), and the turn was restrained to be type 3:5 (Sibanda et al., 1989) due to the glycine at position 4. Models were built with stoichiometries of 4, 5, and 6. Once TMII had been built, the model was extended to include TMI and TMIII by taking the transmembrane region of a single subunit of the topologically similar, inwardly rectifying K^+ channel IRK1 (Stanfield et al., 1994), superposing this onto the β-barrel, and then mapping the respective sequence onto TMI and TMIII, ensuring that the α-helix was oriented such that polar residues pointed toward the center of the pore. Models containing an alternative loop-like topology for TMII were produced interactively, starting from the β-barrel topology, using the program SCULPT version 1.1 (Surles et al., 1994).

The method of orienting the LAOBP-like domain with respect to the transmembrane domain was empirical, relying on the available data (e.g., solvent exposure of the known sites for glycosylation and access to the agonist-binding site). Currently available methodologies for docking (e.g., Kuntz et al., 1994) were not appropriate because some of the residues involved in the interface between the LAOBP-like domains and the transmembrane domains, and LAOBP-like domains of adjacent subunits are omitted. That is, 17 or 18 residues immediately before TMI, 12 or 13 residues immediately after TMIII, and 14 or 17 residues immediately before TMIV did not have homology with the bacterial amino acid-binding proteins and could not be modeled with confidence.

Measurement of the pore diameter

The pore diameter was measured for each of the β-barrel-based models using the program HOLE (Smart et al., 1993). AMBER "united atom" atomic radii (Weiner et al., 1984) and a distance between planes of 0.25 Å were used. The results were inspected visually using the interactive molecular graphics programs InsightII (Biosym) and QUANTA (Molecular Simulations).

Experimental restraints

As many of the available experimental data as possible were considered in generating the sequence alignments and building the model. In the LAOBP-like domain, consensus sites for *N*-glycosylation that have been shown to be glycosylated in native or functional glutamate receptors were constrained to the surface of the protein. These included positions N406 of GluR1 (Hollmann et al., 1994) and N61[453] and N80[473] of Frog KBP (Wo and Oswald, 1995a) in the N-terminal extracellular domain and N265[666] of Frog KBP (Wo and Oswald, 1995a), N720[733] of GluR6 (Roche et al., 1994; Taverna et al., 1994; this corresponds to N326[733] of GFKARα, which is also glycosylated in the native protein; Wo and Oswald, 1994), and N352[759] and N359[766] of GFKARα (Wo and Oswald, 1994, 1995b). (To standardize references to sequence positions, we will refer to the sequence number of the subunit under discussion followed, in brackets, by the corresponding GluR1 number as given in Fig. 2. For example, Gly 200 of GFKARα will be referred to as G200[603]. In referring to GluR1, the number in brackets is omitted. Numbering starts at the beginning of the signal sequence.) A disulfide bond was placed between half-cystines 732 and 787 (GluR1 numbering) for the following reasons: 1) these are the only cysteines absolutely conserved in this domain of the protein, 2) Sullivan et al. (1994) have shown that these residues are involved in redox modulation of NMRA-R1 subunits in a manner reminiscent of the reduction and oxidation of a disulfide bond, and 3) recent observations (Wo and Oswald, unpublished results) have indicated the presence of a disulfide bond between the corresponding residues in the 50 kDa goldfish kainate receptor subunits (GFKARα and GFKARβ). A major consideration was to position the chains such that positive charges were not in the narrowest part of the channel pore. The effects of RNA editing and the results of site directed mutagenesis were also a consideration. The explanation we propose for the selectivity of the Q/R/N site in the β-barrel form of the P-segment requires a specific hydrogen bonding pattern in TMII and, coupled with the need to exclude positive residues from the pore, this defines the position of the second β-strand in a subunit with respect to the first and the position of TMIII in a subunit with respect to TMI.

RESULTS AND DISCUSSION

Sequence alignments

The sequence alignments used for the modeling are shown in Fig. 2. Experimental evidence supporting this alignment comes from site-directed mutagenesis of NMDA and non-NMDA glutamate receptors (Kuryatov et al., 1994; Li et al., 1995; Uchino et al., 1992), which has identified three regions likely to be involved in agonist binding, corresponding to positions 411 to 418, 461 to 465, and 662 to 666 (GluR1 numbering). Our sequence alignment (Fig. 2) differs from that used to produce a preliminary model of the LAOBP-like domain of GluR3 (Stern-Bach et al., 1994) in the following two respects: 1) In our alignment relative to the previously published alignment, the positions of all the bacterial periplasmic amino acid-binding proteins are displaced by two or three residues with respect to all the glutamate receptor sequences between positions 453 and 484 (GluR1 numbering). This does not change the overall quality of the alignment, and one of the important regions determining agonist affinity is positioned near the binding site (corresponding to residues 461 to 465 in GluR1). Mutation of the residue corresponding to K463 in GluR1 decreases the affinity for L-glutamate, but not kainate, in several AMPA receptor subunits (Li et al., 1995; Uchino et al., 1992), and GFKARβ contains alanine at this position and exhibits relatively low L-glutamate affinity (Wo and Oswald, unpublished observations), suggesting that this residue may interact directly with glutamate in the binding site. 2) A large portion (corresponding to residues 666 to 756 in GluR1) of the C-terminal part of the LAOBP-like domain is aligned differently by Stern-Bach et al. (1994). The ability

to form the disulfide bond between half-cystines corresponding to C732 and C787 in GluR1 is the major factor differentiating between the two alignments. In the study of Stern-Bach et al. (1994), the first of these two half-cystines is in a β-strand and points away from the second, thereby resulting in a highly strained molecule when the disulfide bond is formed. Based on our alignment, this disulfide bond can be formed relatively easily. A second consideration is that the glycosylation site at N265[666] in FKBP (Wo and Oswald, 1995a) would line the extracellular vestibule to the pore (an unlikely position) if our models were based on the alignment of Stern-Bach et al. (1994). Using the program PROSA II (Centre for Applied Molecular Engineering, Salzburg, Austria; Sippl, 1993), we found no correlation between the "framework" and the quality of the 3D-1D profiles for all six of the LAOBP-like domain models, implying that side-chain environments in these regions are no better modeled than in the "nonframework" regions.

Stoichiometry

The subunit stoichiometry of non-NMDA glutamate receptors has not been established definitively. Other ligand-gated ion channels are pentamers (Changeux et al., 1992); however, potassium channels (Liman et al., 1992; MacKinnon, 1991) and cyclic nucleotide-gated channels (Root and MacKinnon, 1994), which share some homology with the channel domain of glutamate-gated ion channels, are tetramers. Both sedimentation analysis and chemical cross-linking have been employed to study the oligomeric state of the 100 kDa iGluRs and 40–50 kDa kainate receptors, and the results have generally been interpreted as an indication of pentameric structure (Blackstone et al., 1992; Brose et al., 1993; Wenthold et al., 1992; Wu and Chang, 1994), similar to nicotinic acetylcholine receptors. Furthermore, the relative abundance of GluR2 mRNA in determining the Ca^{2+} permeability of AMPA receptors is consistent with the assumption of a pentameric structure (Geiger et al., 1995). Nevertheless, the data are not unambiguous. For example, previous chemical cross-linking generated a rather diffuse pattern of high-molecular-weight components in the unreduced samples (Brose et al., 1993; Wenthold et al., 1992), and velocity sedimentation analysis could be consistent with either a tetramer or a pentamer (Blackstone et al., 1992; Henley and Oswald, 1988; Wu and Chang, 1994). We have, therefore, generated three sets of β-barrel-based models assuming a tetrameric, pentameric, and hexameric structure to investigate systematically the different possible stoichiometries on the structure. Apart from the number of subunits, the main differences between the three sets of models arise from subtleties in the packing of the extracellular domains and in the size and shape of the channel. The size of the channel predicted in comparison with the available experimental evidence lends support to a pentameric structure, although a tetrameric structure cannot be ruled out (see below).

LAOBP-like domain

General characteristics of structure and orientation with respect to the membrane

Although most of the LAOBP-like domain corresponds to the bacterial periplasmic amino acid-binding proteins, there are 17 or 18 residues immediately before TMI and 12 or 13 residues immediately after TMIII that do not. These residues were omitted from the model because no information was available to allow us to model this portion of the protein with confidence. We also had little confidence in modeling the region between the C-terminal α-helix in the LAOBP-like domain and TMIV, because of the paucity of available information; the structures of LAOBP and HBP extend beyond this position in the form of a C-terminal loop. Because this region contains one of the half-cystines (position C787 in GluR1) that form the disulfide bridge, we modeled this region just (i.e., three residues) beyond this half-cystine, omitting the remaining residues. The AMPA receptors (GluR1 to 4) have modules (FLIP/FLOP) that can be alternatively spliced in the TMIII/TMIV loop (Sommer et al., 1990). This module is near the point where the extracellular domain enters the membrane at TMIV and was not included in the modeling. The substitution of the FLOP sequence (motif N-$(X)_{21}$-GGGD) for the FLIP sequence (motif S-$(X)_{21}$-KDSG) accelerates dramatically the kinetics of desensitization in the presence of glutamate but not kainate. The glycines in FLOP confer flexibility on this region, suggesting that the functional differences between the FLIP and FLOP forms may be a result of a differential flexibility of this portion of the structure. Because this region of the protein serves as a linker to TMIV, it could play an important role in transferring the conformational change caused by the binding of agonist into the membrane-embedded portion of the channel pore. This is interesting, particularly in light of the hypothesis that a hinge-bending motion of the extracellular domain can lead to a distortion of the portion of the protein embedded in the membrane, giving rise to channel activation and desensitization.

The model of the LAOBP-like domain was positioned empirically with respect to both the membrane and its symmetry-related copies such that the consensus glycosylation sites were solvent accessible (Fig. 3 *D*), the agonist binding site was accessible, the distance between the end of the N-terminal section of the LAOBP-like domain and TMI was within a reasonable range, the distance between TMIII and the start of the C-terminal section of the LAOBP-like domain was within a reasonable range, and the domain was as close to the pore as possible without overlapping sterically with its symmetry-related copies in both the apo and holo forms. In the resulting orientation, the long axis of the molecule was parallel to the surface of the membrane. Although a unique solution to the positioning of this domain is not possible with the currently available data, this alignment is not inconsistent with any available experimental restraints and is, in fact, constrained considerably by the experimental results. There is a region of this domain

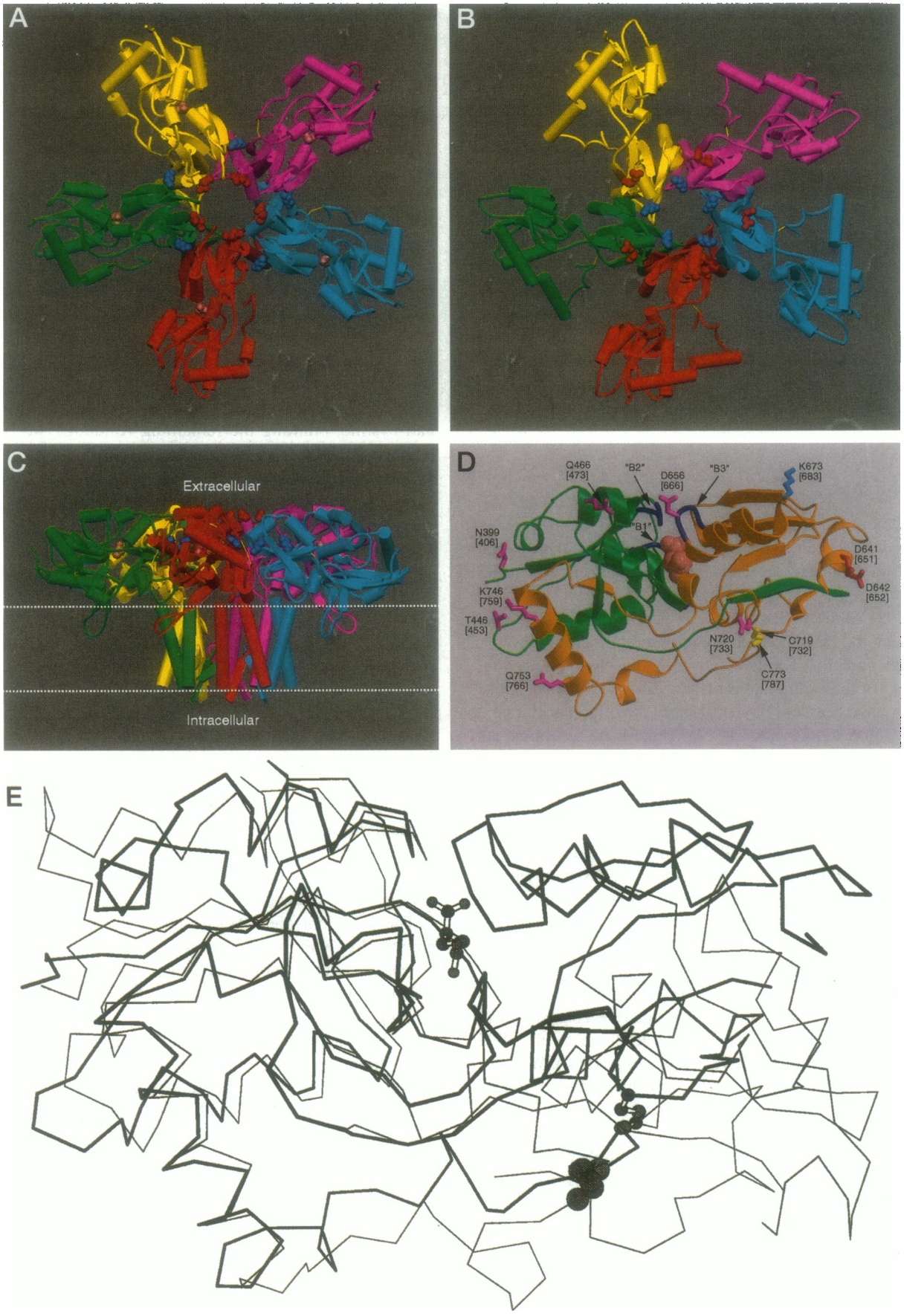
A
B
C
Extracellular
Intracellular
D
Q466 [473]
"B2"
D656 [666]
"B3"
K673 [683]
"B1"
N399 [406]
D641 [651]
D642 [652]
K746 [759]
T446 [453]
N720 [733]
C719 [732]
Q753 [766]
C773 [787]
E

which, in our models, passes into the membrane (residues 423 to 433 in GluR1; see Fig. 3 *C*). Although this is unlikely to be correct, it was not modified because it does not affect our conclusions and it is unclear how it should be modeled.

Binding of agonist

Based on homology with bacterial periplasmic amino acid-binding proteins, and consistent with site-directed mutagenesis (Kuryatov et al., 1994; Li et al., 1995; Uchino et al., 1992) and the generation of chimeric subunits (Stern-Bach et al., 1994), agonist is likely to bind in the cleft between the two lobes. Three "hot spots" affecting the binding of agonist to both non-NMDA and NMDA receptors have been identified (Fig. 3 *D*). These include (B1) a region near the beginning of the N-terminal LAOBP-like domain (VTTIXE; [411–416]), (B2) a region approximately 40 residues C-terminal to B1 in the N-terminal LAOBP-like domain (DGXYG; [461–465]), and (B3) a sequence near the beginning of the TMIII/TMIV loop region of the LAOBP-like domain [662–667]. Using the sequence alignment shown in Fig. 2, these "hot spots" all fall within the agonist-binding region in the resulting three-dimensional models.

Because both the glutamate of B1 (VTTIXE; Uchino et al., 1992) and the X of B2 (DGXYG; Li et al., 1995; Uchino et al., 1992) are important determinants of glutamate affinity, glutamate has been oriented in the binding site so that its amino nitrogen interacts with the E of B1 (E416 in GluR1) and its α-carboxyl interacts with K or R of B2 (DG {K or R} YG; K463 in GluR1). Of particular interest is the observation that mutation of these residues has a differential effect for different agonists. These differential effects are not easily explained on the basis of our models, but it is important to note that ligands with even small variations in structure can orient differently in a binding site (e.g., Ealick et al., 1991). In any event, activation of a mouse AMPA receptor by AMPA, glutamate, and kainate is decreased by two or more orders of magnitude when E of B1 (E416 in GluR1) is mutated to Lys (Uchino et al., 1992). The residue in the X position of DGXYG, however, affects activation by glutamate and AMPA but not by kainate, in that a positively charged residue (K or R) is required for a higher apparent affinity. Although it cannot be definitively determined from a set of models such as these, the possibility exists that since, in contrast to glutamate and AMPA, the amide and α-carboxyl of kainate, as well as the side chain, are held in relatively rigid positions because of the ring structure, kainate may not have the flexibility necessary to interact with the X group of the DGXYG B2 sequence. Another potentially interesting position is that corresponding to R499 in GluR1, which is conserved in all non-NMDA glutamate receptors. This position in a mouse AMPA receptor was mutated by Uchino et al. (1992), and any changes in this position resulted in no measurable activity in an oocyte system. The reasons for this lack of activity could have been a massive decrease in the binding affinity, interference with the signal transduction mechanism, interference with the folding of the protein, and/or interference with the expression of the protein on the cell surface. In any event, the model predicts that this residue would be present in the binding site and potentially interact with the γ-carboxyl of glutamate. It is unlikely that R499 would interact with the "main chain" carboxyl of glutamate because, in that case, an interaction of the amino group of glutamate with E416 would no longer be possible.

The third "hot spot," B3, is in the loop between TMIII and TMIV, as suggested by the generation of chimeras between GluR3 and GluR6 (Stern-Bach et al., 1994) and by site-directed mutagenesis of an NMDA receptor (Kuryatov et al., 1994). The exact amino acids that might form part of the binding site in non-NMDA glutamate receptors are not clear from these studies. Mutation of S267[668] in FKBP decreases the binding affinity for kainate by approximately threefold (Wo and Oswald, 1995a), and the two residues important for coactivation by glycine in an NMDA receptor are within 5 Å of glutamate as positioned in the models. As shown in Fig. 4, the position corresponding to R706 in GluR1 faces into the binding site and thus could be a site of interaction with ligand. In particular, assuming that kainate and domoate can align in the binding site in the same orientation as glutamate, the position corresponding to R499 in GluR1 noted above might interact with a "side chain" carboxyl of kainate and domoate; whereas the position corresponding to R706 in GluR1 could interact with the second "side chain" carboxyl of domoate, which is absent in kainate. This could explain the higher affinity for domoate than for kainate.

FIGURE 3 A schematic representation of the pentameric structure of the bacterial periplasmic amino acid binding protein-like domain and the "inserted" voltage-gated K^+ channel-like domain for GluR6. (*A*) Looking down onto the holo form from the extracellular side; (*B*) looking down onto the apo form from the extracellular side; and (*C*) looking perpendicular to the axis of the channel of the holo form with the extracellular domain of the channel above the membrane. The approximate extent of the membrane is shown with dashed white lines. D641[651] and D642[652] (*red*), K673[683] (*blue*), and agonist in the holo form (*pink*) are shown in CPK. (*D*) An enlargement of one of the LAOBP-like domains from *A* showing the three charged residues, together with the glycosylation sites discussed in the text (*purple*), the disulfide bond (*yellow*) and the three regions thought to comprise the agonist binding site (B1, B2, and B3). The portion of the structure arising from the N-terminal extracellular domain is shown in green, and that arising from the sequence between TMIII and TMIV is shown in copper. The glycosylation sites shown are not only those found in GluR6, but also those that are known to exist in other non-NMDA receptors in the region of the protein represented. Thus this representation is used to illustrate the restraints used to build the model rather than the actual glycosylation sites of GluR6. (*E*) Cα trace of the holo (*thick lines*) and apo (*thin lines*) LAOBP-like domains of GluR6, superposed on the Cα atoms of the lobe containing the N- and C-termini. The glutamate agonist and disulfide bridge are shown in ball-and-stick representation; the balls are larger for the disulfide bridge in the apo form. *A* through *C* were generated using SETOR (Evans, 1993), *D* was generated using MOLSCRIPT (Kraulis, 1991) and RASTER3D (Merritt and Murphy, 1994), and *E* was generated using MOLSCRIPT.

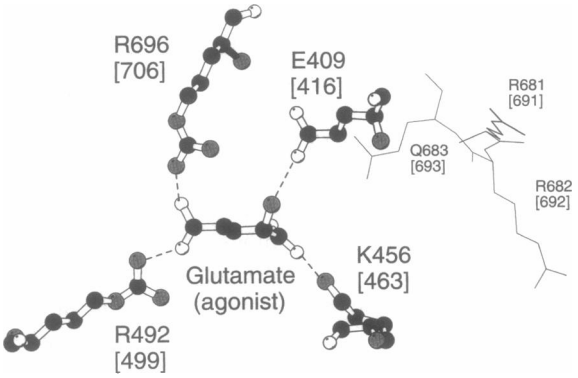

FIGURE 4 Enlarged view of the residues proposed to be important for the interaction of GluR6 with glutamate. Carbon is shown in black, nitrogen in gray, and oxygen in light gray; hydrogens are omitted for clarity. Possible glutamate/protein interactions are shown as dashed lines. This figure was generated using MOLSCRIPT (Kraulis, 1991).

An important question is, what determines the relative affinities for AMPA and kainate in the AMPA receptors (GluR1 to 4) and the kainate receptors (GluR5 to 7, KA-1 and 2, and the kainate binding proteins)? One clue comes from the chimeras produced between GluR3 and GluR6 (Stern-Bach et al., 1994). One chimera in which the N-terminal extracellular domain came from GluR6 and the loop between TMIII and TMIV came from GluR3 exhibited high affinity for both kainate and AMPA. By searching the sequences to find residues near the agonist-binding site that are conserved among AMPA receptors and among kainate receptors, but which differ between the two, we propose that the residues AEP (691–693 in GluR1) in the AMPA receptors may be an important determinant of affinity for AMPA (see Fig. 4). The difference in affinity for kainate between kainate and AMPA receptors is much smaller (approximately fourfold), and the correlation with structure is not obvious from either the sequence or the models.

Disulfide bonding

The disulfide bonding pattern places important constraints on the structure. Cys 307[732] is disulfide bonded to Cys 358[787] in GFKARβ (Wo and Oswald, unpublished results), and the corresponding two residues (Cys 744 and Cys 798) are involved in the redox regulation of NMDA-R1 subunits (Sullivan et al., 1994). This is likely to be a general pattern in all glutamate-gated ion channels, because these residues are conserved in all iGluRs (see Fig. 2). The characteristics of this regulation are reminiscent of the breaking and reformation of a disulfide bond. The position of the disulfide has important implications for the orientation of the two lobes forming the binding site. Modeling GFKARα by homology with LAOBP in the presence and absence of agonist without the explicit inclusion of the disulfide indicates that these two residues are in close proximity in the unbound model but are separated by more than 20 Å in the bound model. In our models of the holo forms, the conformational changes required to form the disulfide bond are accommodated almost entirely in the two "loops" in which the respective cysteines occur. Because the final structure is dependent upon the procedures used to generate the model, it is difficult to predict exactly how the disulfide bond will affect the overall conformation, but it is likely that the formation of a disulfide bond affects more than the two loops that contain the cysteines. Because in the bacterial binding proteins, the two lobes close in a hinge-like motion upon agonist binding (Fig. 3 *E*), the presence of a disulfide in this position could restrict this motion, leaving the bound form with a slightly more "open" binding site. Evidence for this model comes from studies of [^{3}H]kainate binding to GFKARα and GFKARβ. [^{3}H]Kainate binds with an affinity approximately threefold greater in the presence than in the absence of reducing agents (Wo and Oswald, unpublished observations). A decrease in the dissociation rate can account entirely for this difference. Thus, by reducing this disulfide, the lobes would potentially be less constrained and could approach the more "closed" conformation characteristic of lysine bound to LAOBP. This could in turn impede the dissociation of agonist, thus increasing affinity.

Binding and signal transduction

In bacterial periplasmic amino acid-binding proteins, ligand binding is accompanied by a closing of the two lobes in a hinge-like motion. If a similar transition occurs in glutamate receptors, then this is likely to be part of the signal transduction pathway that leads to channel opening. At the resolution of this model, the details of this process cannot be determined, particularly because of the fact that portions of the extracellular domain (residues 525 to 538, 637 to 646, and 791 to 807 in GluR1) must be left undetermined, because they are outside of the regions of homology with bacterial proteins and potassium channels. However, one general and one specific point can be made based on the model. First of all, the transition between the bound and unbound states, assumed to be a closing of the gap between the two lobes, could be propagated to changes in the orientation of the helices forming the membrane-spanning regions (TMI, TMIII, and TMIV). More specifically, the transition between the bound and unbound forms results in a change in the orientation of two sets of highly conserved amino acids of opposite charge. In GluR1 numbering, this corresponds to E651 and D652, and K683. In the unbound form, K683 would be near the extracellular opening of the channel, impeding the flow of cations into the channel (Fig. 3). When agonist is bound and the lobes are closed, K683 is moved away from the opening and E651 and D652 are placed near the opening of the channel (Fig. 3). This negative charge would attract cations to the channel in a manner analogous to the ring of negative charges in nicotinic acetylcholine receptors (Imoto et al., 1988).

Membrane domains

Choice of segment and secondary structure

The three transmembrane domains are largely defined from experimental constraints that determine the transmembrane location of various segments of the primary sequence (Bennett and Dingledine, 1995; Hollmann et al., 1994; Wo and Oswald, 1994, 1995a,b,c; Wood et al., 1995). This topological analysis is completely consistent with the hydropathy profile, which indicates three very hydrophobic regions of approximately 20 amino acids, in addition to the signal sequence (Wo and Oswald, 1995c). Furthermore, the positions in the sequences of the transmembrane domains were determined using MEMSTAT (Jones et al., 1994) and TMAP (Person and Argos, 1994), which rely on information from known transmembrane helical segments. In the absence of conflicting experimental evidence, consistent with secondary structure prediction using the program PHD (Rost and Sander, 1994), and consistent with the predictions derived from MEMSTAT and TMAP, TMI, TMIII, and TMIV were assumed to be helical. Because TMIV is completely hydrophobic in GFKARα, GFKARβ, FKBP, KA1, and KA2, it was assumed that this is positioned away from the pore, with TMI and TMIII lining the extracellular end of the pore. In the absence of additional evidence concerning the placement of TMIV, it was left out of the model at this stage, but a discussion of its possible structure and orientation is included at the end of this section. Although some ambiguity exists in defining the length of TMI and TMIII, the consensus we used is shown in Fig. 2. The position in the sequence of the P-segment (TMII), its length, and its secondary structure were more difficult to predict than those of TMI and TMIII. Because the P-segment is easier to model as a β-barrel than in any other form and most experimental data are consistent with such a topology, an antiparallel β-barrel was adopted as an initial working model. The β-barrel starts immediately after the totally conserved glycine (G596 in GluR1) and ends immediately before the totally conserved proline (P607 in GluR1). Although both glycine and proline tend to act as β-strand "breakers," the presence of both these residues in the β-strands of some of the sequences (Fig. 2) does not preclude their existence—a search of the IDITIS database of protein structures (Oxford Molecular) reveals that there are in excess of 1000 instances of both glycine and proline occurring in β-strands. An alternative loop-like topology for the P-segment, based on the β-barrel, was also investigated, as was a loop-like topology based on recent findings for voltage-gated K^+ channels.

Size of the pore

Because the current experimental data do not definitively determine the stoichiometry of glutamate-gated ion channels, symmetrical models with the P-segment in the form of a β-barrel comprising 4, 5, and 6 subunits were generated. The minimum radius of the channel in each of the 7 to 11 final models for each stoichiometry was determined with HOLE, and the data are given in Table 1 (note that these results are for the β-barrel topology). The size of the pore is highly dependent upon the detailed topology of the P-segment and the side chains. However, based purely on size constraints, the tetramer would appear to be too small to accommodate Na^+ and Ca^{2+} permeability through the channel, and the hexamer could potentially freely pass Mg^{2+}. Based on these considerations, the pentamer would be the most likely stoichiometry. However, a tetramer cannot be ruled out at this point; indeed, voltage-gated channels are either tetramers (K^+ channels and cyclic nucleotide-gated channels) or have four internal repeats (Na^+ and Ca^{2+} channels). A further note of caution comes from the observation that changing only three residues in the P-segment of a cyclic nucleotide-gated channel results in a significant difference in apparent pore size (Goulding et al., 1993). Nevertheless, if one assumes that the NMDA receptors have a structure similar to the non-NMDA receptors, the overall size of the pentamer is entirely consistent with the estimation of the pore size of NMDA receptors with organic cations (Villarroel et al., 1995; Zarei and Dani, 1995). The narrowest region of the pore was estimated to be approximately 5.5 Å, and the outer region of the pore (assumed here to be the portion of the pore lined by TMI and TMIII) was found to be greater than 7.3 Å. As described below, our final models contain a loop-like structure and thus deviate from the β-barrel. The modified structure was produced manually, rather than automatically, which precludes systematic sampling of the range of pore sizes available for a given stoichiometry. Because the final models are a modification of the β-barrel discussed above, to a reasonable first approximation, the discussion of stoichiometry relating to the β-barrel also applies to the loop-like structure.

Position and role of the Q/R switch

(In this section and subsequent sections, only homomeric glutamate receptors will be considered in the analysis. Heteromeric receptors are undoubtedly of considerable physiological importance, but our relative ignorance of the complexities associated with the quaternary structure precludes any detailed analysis.) An important consideration in building the model was the position of the residue known to affect channel conductance in a number of iGluRs. This

TABLE 1 Relationship between the size of the narrowest part of the pore of GluR6 and its stoichiometry

Stoichiometry	No. of models	Range of width of narrowest part of pore (Å)	Average width (Å)
Tetramer	7	0.6 to 2.8	1.8 ± 0.8
Pentamer	11	1.2 to 6.8	4.8 ± 1.8
Hexamer	7	4.8 to 9.0	7.8 ± 1.4

Note that all pore sizes were determined using the program HOLE (Smart et al., 1993), based on β-barrel topology for the P-segment.

position in GluR6 and GluR2 (residue 600 in GluR1) can be changed from a Q to an R by RNA editing (Sommer et al., 1991) and is known to be involved in the blockade of NMDA receptors by Mg^{2+} (N598 of NMDA-R1; Burnashev et al., 1992b). Cysteine-scanning mutagenesis of NMDA receptor channels supports the exposure of this residue, because the Cys residue replacing the key Asn (equivalent to the Q/R site of AMPA receptors) in TMII is highly accessible to methanethiosulfonate (MTS) derivatives (Kuner et al., 1995). However, this residue would clearly not be exposed to the narrowest part of the conductance pathway in the R form, because the positive charge would impede the flow of ions through the channel. It is more likely that at least the side chain in the R form is shielded by the protein to some extent. This would provide an efficient mechanism for changing the conformation of the P-segment and/or residues around the P-segment. One possibility that has been suggested (Dingledine et al., 1992) is that the arginine can interact with the negatively charged residue (D or E) found four residues C-terminal (see Fig. 2 and below). In non-NMDA receptors, the Q form displays characteristic double rectifying behavior, with currents for potentials around zero millivolts exhibiting a very shallow slope and weak outward currents observed only at high positive voltages. In the R form, however, the *I/V* curve is either linear or outwardly rectifying (e.g., Verdoorn et al., 1991).

Although many of the subtle features would require more detailed knowledge of the structure and dynamics of the channel, the model of the P-segment based on a β-barrel can account for much of the overall behavior of the channel. In the Q form, the glutamine could be exposed to the channel lumen and provide a ligand for hydrogen bonding that could be involved in the dehydration of cations passing through the channel. This could provide a weak binding site for divalent cations such as Ca^{2+}, making the channel slightly more selective for divalents but also less permeable to them. Note that the loss of the waters of hydration from Ca^{2+} involves a significantly larger energetic penalty than for Na^{+} (e.g., Hille, 1984). This difference can be compensated if the waters of hydration can be replaced by polar groups, particularly hydroxyl groups and negatively charged groups from the protein, as the ion passes through the pore. This is supported by the higher currents observed in the presence of high Na^{+} than of high Mg^{2+} or high Ca^{2+} (Burnashev et al., 1992a). With the switch from Q to R, the effect of Q on dehydration of divalent cations would be lost, and the channel should become relatively less permeable to Ca^{2+}. Again, this is observed for AMPA receptor channels (in particular GluR2), but not necessarily for GluR6 (Köhler et al., 1993). GluR6 (as well as the other kainate receptors GluR5–7 and KA-1 and KA-2) differ from the AMPA receptors (GluR1–4) in the presence of a Ser versus Cys three residues C-terminal to the Q/R site. As will be described below, the relative Ca^{2+} permeability is determined by a combination of editing in TMI and TMII. For GluR6, the relative Ca^{2+} permeability is not greater in the Q form than the R form. One potential reason for this is that Q could hydrogen bond to the Ser[603], removing its contribution to the dehydration of divalents, in a manner similar to the salt bridge that could form between R and the negatively charged residue described above.

Considering now the double rectification behavior, a site four residues C-terminal to the Q/R[600] site is either Asp or Glu[604] in all non-NMDA receptors that form functional homomeric channels. One possibility is that this negative charge serves as a divalent cation-binding site in, but away from, the narrowest part of the pore, as is the case with cyclic nucleotide-gated channels (Eisman et al., 1994; Root and MacKinnon, 1993) and could be the case with modified voltage-gated K^{+} channels (Heginbotham et al., 1992). This could then impede the flow of both outward and inward currents by a mechanism similar to channel blockade (Bowie and Mayer, 1995). The small inward and outward currents at high potentials could arise from a breakthrough phenomenon seen with small semipermeable channel blockers at high membrane potentials (Woodhull, 1973). In the R form, the protein would have to mask the presence of the positive charge to allow positive ions to flow through the channel. As noted above, the most likely candidate for this masking effect is the negative charge at position 604 (Fig. 5 *A*). A salt bridge could then form between the arginine (in an adjacent subunit) and the negatively charged residue, masking not only the positive charge but also the negative charge. This would in turn remove the divalent cation-binding site postulated to be present in the Q form, allowing both outward and inward currents to flow more readily. This is, in fact, what is observed (Burnashev et al., 1992a; Hume et al., 1991).

However, the relatively buried location of the D/E[604] site (Fig. 6 *A*), combined with a paucity of oxygen atoms to coordinate with a Ca^{2+} ion binding to this site, is an indication that the proposed β-barrel-based model of the P-segment may be incorrect. We therefore modified the β-barrel-based model to make the D/E[604] site more accessible to the pore (Fig. 6 *B*), producing a loop-like topology for the P-segment (Fig. 5 *B*). Electrostatic calculations on GluR1, using the program DELPHI (Nicholls and Honig, 1991), indicate that a cation is far more likely to bind to the D/E[604] site in the loop conformation than in the barrel conformation. Although it is possible that this modified topology could be an antiparallel β-barrel with a seven-residue loop, rather than a five-residue turn, a β-barrel is thought unlikely because this could position the D/E[604] close to the center of the pore, which would be undesirable in its proposed Ca^{2+}-bound form.

The P-segments of the iGluRs and voltage-gated K^{+} channels show significant sequence similarity (Wo and Oswald, 1995b; Wood et al., 1995). Therefore, in light of recent studies on the topology of voltage-gated K^{+} channels (Kurz et al., 1995; Lu and Miller, 1995; MacKinnon, 1995; Pascual et al., 1995), the available data for iGluRs were compared with the emerging topology of voltage-gated K^{+} channels. A schematic of a model based on the current view

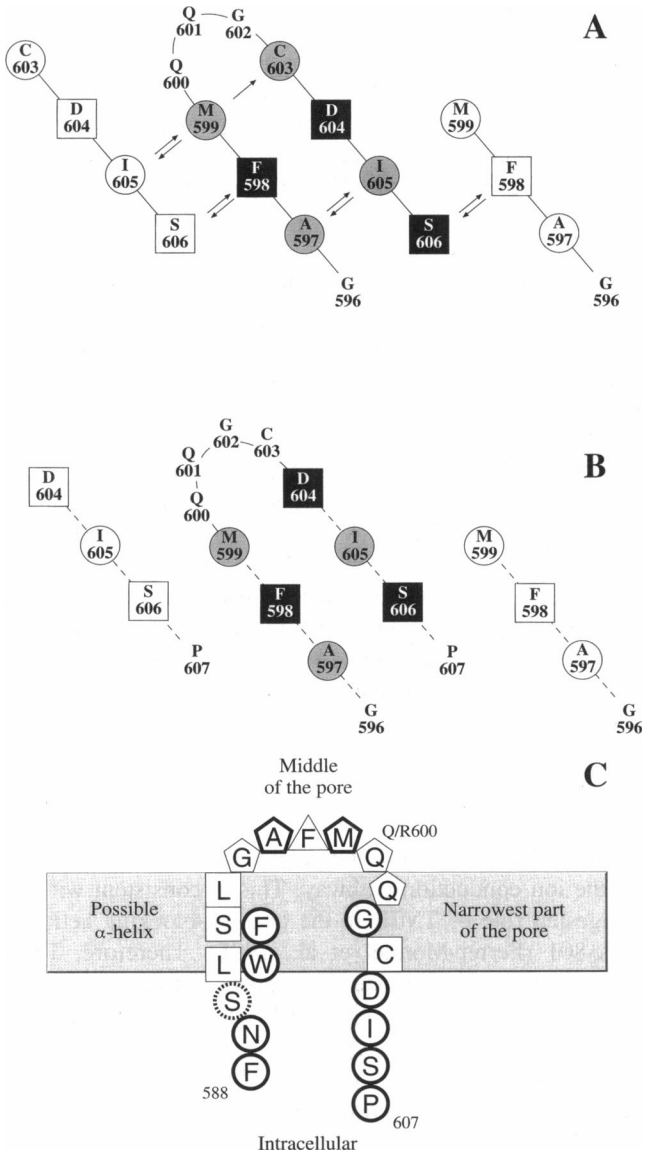

FIGURE 5 Schematic of (*A*) the β-barrel topology for GluR1 (hydrogen bonds are shown as *black arrows*); (*B*) the modified loop structure for GluR1; (*C*) the P-segment of GluR1 based on the current view of the structure of the corresponding region of K^+ channels. In *A* and *B* the P-segment from one subunit is shown, with one strand from adjacent subunits on either side (the central P-segment is highlighted with *gray circles* and *black squares*). The residues surrounded by a circle point into the channel and those surrounded by a box point away from the channel. In *A*, residues M599 to C603 are in the 3:5 turn. In *B*, the residues are connected by a dashed line to emphasize that these are not in a β-strand topology. In *C*, the residues shown surrounded with a thick line are likely to line the pore. Circles correspond to those residues in voltage-gated K^+ channels shown to line the pore (the *dashed circle* on S590 denotes that it appears to be somewhat buried; Lu and Miller, 1995). Pentagons correspond to residues that have been mutated in GluR3 (Dingledine et al., 1992); those with thick lines correspond to "killer" mutations and therefore are likely to lie close to the ion conduction pathway. A triangle denotes a residue for which there is no information about its position. Note that in this topology, no negative charge is present to neutralize the two R mutation sites (598 and 600) in the loop in the middle of the pore.

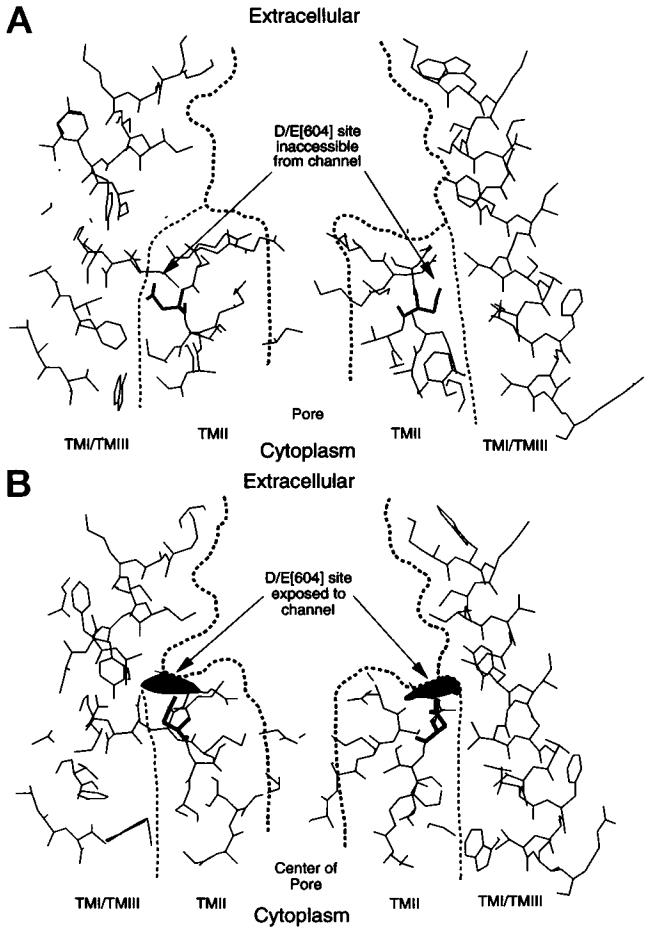

FIGURE 6 Cross section of (*A*) the β-barrel topology and (*B*) the modified loop structure for the pentameric form of GluR1. Note that the negatively charged residue is exposed to the channel in the loop structure (*B*), as shown by the black patch, which denotes the solvent-accessible surface of this residue, but is inaccessible to it in the β-barrel (*A*). The pore is indicated by a thicker dashed line, and the region occupied by the P-segment is delineated by a thinner dashed line.

of K^+ channel structure is shown in Fig. 5 *C*. This model places the D/E[604] site near the cytoplasmic face of the channel, which is not inconsistent with available data, but it is now in a position that precludes its interaction with R600 (i.e., the Q/R site), placing a positive charge in the narrow region of the pore. Thus, although both K^+ channels and iGluRs seem to have pore loops, the details of the structure of the loops are likely to differ.

Site-directed mutagenesis of the channel and possible orientation of the P-segment

Dingledine et al. (1992) mutated a number of TMII residues of GluR3 to Arg to assess the similarity of the mutation to mutations at the Q/R site. In GluR3 numbering, A609R and M611R (i-3[597] and i-1[599], respectively, relative to the Q/R site) both produced inactive homomeric receptors and were killer mutations in the

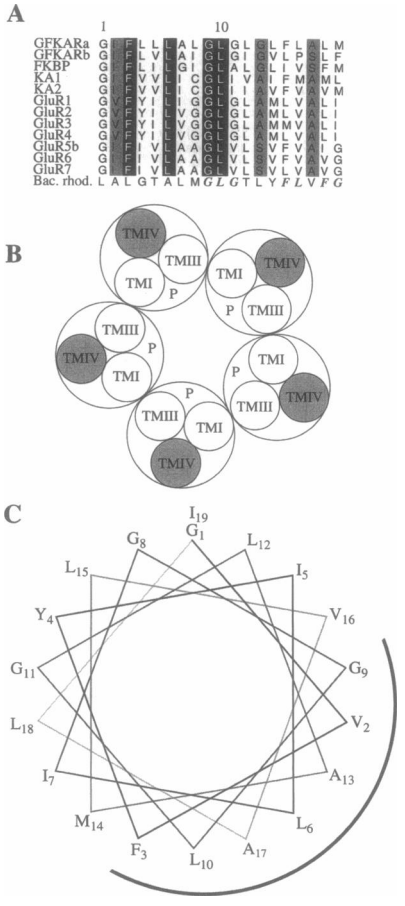

FIGURE 7 (*A*) Alignment of TMIV for various iGluRs and comparison with the first transmembrane spanning region of bacteriorhodopsin. The residues in bacteriorhodopsin with similarities to the iGluRs are shown in italics. Absolutely conserved positions are shown white on black. Other positions thought to form the interface with the remainder of the protein are shown with a gray background. (*B*) A schematic showing a plausible arrangement of transmembrane segments for a pentamer. Note that no data are available to position TMIV relative to the other subunits, so that other arrangements are also possible. (*C*) The helical wheel is shown for the GluR1 sequence of TMIV, and the semicircle highlights the region proposed to interact with TMI and TMIII.

sense that no current was observed when they were expressed with other GluR subunits. G608R and Q613R (i-4[596] and i+1[601], respectively, relative to the Q/R site) produced inactive homomeric receptors that functioned in a complex with GluR1. Both our β-barrel and loop-like models are consistent with these observations. Because of the turn or loop, respectively, at the tip of the P-segment, the Q613R [601] mutant could still form a salt bridge with the D/E site. This would likely change the orientation of the segment, but may not destroy channel activity. The G608R [596] mutant would be outside of the P-segment. The two killer mutations (A609R [597] and M611R [599]) would put a positive charge in the narrow part of the channel in both topologies, thus destroying channel activity.

Potential role of TMI in ion conduction

An essential feature of a pore loop is the fact that other membrane-spanning regions are likely to form a part of the conductance pathway. To a first approximation, the models are consistent with the effects of RNA editing of residues in TMI of GluR6 (Köhler et al., 1993). In the case of GluR6, RNA editing can convert T536[543] to V and Y540[547] to C. These residues are near the extracellular side of the channel and are separated by one turn of an α-helix; thus, they could be exposed to the lumen of the channel but be outside the narrow portion of the channel. RNA editing of TMI of GluR6 produces only modest changes in the *I/V* relationships of the channel. The interesting differences are in the relative Ca^{2+} permeability. When the Q/R site of TMII is in the R form, RNA editing of TMI has no effect on relative Ca^{2+} permeability; whereas when it is in the Q form, the edited channel (V, C) has a lower relative permeability than the unedited channel (I, Y; Köhler et al., 1993). One possible explanation for this difference could be that Q[600] may hydrogen bond to Y[547], exposing the Ser[603], which is in the narrow portion of the channel. This Ser residue could then provide a binding site for Ca^{2+}, increasing the relative permeability.

Position of TMIII

TMIII is modeled as an α-helix and is predicted to form part of the ion conduction pathway. This is consistent with the suggested role of TMIII in the channel-blocking action of MK-801 (Ferrer-Montiel et al., 1995). Therefore, TMIII was oriented to maximize the exposure of polar groups to the pore. This suggested a possible hydrogen bonding interaction between the Arg at the Q/R[600] site and the conserved Tyr[630] in TMIII, in addition to the proposed ionic interaction between this Arg and the acidic site [604] in TMII. In the absence of other interactions between TMIII and the remainder of the structure, the hydrogen bond was included as an additional restraint, thereby orienting TMIII with respect to TMII. Note that in this arrangement, one amine group of the arginine side chain would form the salt bridge referred to above and the other could participate in the hydrogen bond. It should be stressed, however, that no evidence is currently available to assess whether this hydrogen bond is actually formed in the protein.

Structure and orientation of TMIV

The models predict that TMIV does not line the pore, and because of uncertainties as to how it may interact with the other transmembrane domains, it was omitted from the model. Nevertheless, analysis of the sequence indicates several interesting features that may suggest qualitatively its structure and relative orientation. TMIV is relatively rich in glycine and may not be expected to be α-helical. However, a BLAST search (Altschul et al., 1990) using the GluR1 TMIV sequence showed significant homologies with the

first transmembrane segments of bacteriorhodopsin and the photosynthetic reaction center, both of which are α-helical and rich in glycine (see Fig. 7 *A*; Deisenhofer et al., 1995; Henderson et al., 1990). Cautiously making the assumption that TMIV is α-helical, we show a helical wheel of the sequence in Fig. 7 *C*. Using the numbering from the sequence alignment in Fig. 7 *A*, the face of the helix comprising residues 3, 10, 17, 6, 13, 2, and 9 is a strong candidate for the interaction with TMI and TMIII. The reasoning is that 1) positions 3, 10, 6, and 9 are absolutely conserved; 2) position 2 has only very conservative substitutions; 3) positions 17 in GFKARβ and FKBP, and 13 in GluR5–7, contain the only polar residues found in TMIV; and 4) the remainder of the segment is very hydrophobic and not well conserved, suggesting that it contacts the lipid. One possible orientation of TMIV with respect to the other transmembrane segments is shown in Fig. 7 *B*.

SUMMARY

Based on homology modeling and using constraints such as the position of sites for glycosylation and the disulfide bonding pattern, we have developed relatively detailed models of the three-dimensional structure of two important domains (i.e., the agonist binding site and the ion channel) of non-NMDA glutamate receptors. The models represent an initial guess for the structure of two important regions of non-NMDA glutamate receptors and are consistent with the available data in the literature. As in any modeling study, the result is no substitute for a high-resolution three-dimensional structure; however, the insights obtained suggest a number of avenues for further study and form a framework for rational strategies for further site-directed mutagensis.

MJS is a Royal Society University Research Fellow. ZGW was supported by a PhRMA Foundation advanced predoctoral fellowship. This work was supported in part by grants from the National Science Foundation (IBN-9309480), the John Simon Guggenheim Memorial Foundation to REO, and the Wellcome Trust (042989/Z/95/Z) to MJS. The coordinates will be submitted to the Brookhaven Protein Data Bank and are available at http://web.vet.cornell.edu/pubic/pharmacology/pdbfiles.html.

REFERENCES

Abola, E. E., F. C. Bernstein, S. H. Bryant, T. F. Koetzle, and J. Weng. 1987. Protein data bank. *In* Crystallographic Databases—Information Content, Software Systems, Scientific Applications. F. H. Allen, G. Bergerhoff, and R. Sievers, editors. Data Commission of the International Union of Crystallography, Bonn, Cambridge, Chester. 107–132.

Altschul, S. F., W. Gish, W. Miller, E. W. Myers, and D. J. Lipman. 1990. Basic local alignment search tool. *J. Mol. Biol.* 215:403–410.

Barton, G. J. 1993. ALSCRIPT: A tool to format multiple sequence alignments. *Protein Eng.* 6:37–40.

Bennett, J. A., and R. Dingledine. 1995. Topology profile for a glutamate receptor: three transmembrane domains and a channel-lining re-entrant membrane loop. *Neuron.* 14:373–384.

Bernstein, F. C., T. F. Koetzle, G. J. B. Williams, E. F. Meyer, M. D. Brice, J. R. Rodgers, O. Kennard, T. Shimanovichi, and M. Tasumi. 1977. The protein databank: a computer based archival file for macromolecular structures. *J. Mol. Biol.* 112:535–542.

Blackstone, C. D., S. J. Moss, L. J. Martin, and R. Huganir. 1992. Biochemical characterization and localization of a non-NMDA receptor in rat brain. *J. Neurochem.* 58:1118–1126.

Blundell, T. L., D. Carney, S. Gardner, F. Hayes, B. Howlin, T. Hubbard, J. Overington, D. A. Singh, B. L. Sibanda, and M. Sutcliffe. 1988. Knowledge based protein modelling and design. *Eur. J. Biochem.* 172: 513–520.

Bowie, D., and M. L. Mayer. 1995. Inward rectification of both AMPA and kainate subtype glutamate receptors generated by polyamine-mediated ion channel block. *Neuron.* 15:453–462.

Brose, N., G. P. Gasic, D. E. Vetter, J. M. Sullivan, and S. F. Heinemann. 1993. Protein chemical characterization and immunocytochemical localization of the NMDA receptor subunit NMDA R1. *J. Biol. Chem.* 268:22663–22671.

Brunger, A. T. 1992. Xplor manual version 3.0.

Burnashev, N., H. Monyer, P. H. Seeburg, and B. Sakmann. 1992a. Divalent ion permeability of AMPA receptor channels is dominated by the edited form of a single subunit. *Neuron.* 8:189–198.

Burnashev, N., R. Schoepfer, H. Monyer, J. P. Ruppersberg, W. Günther, P. H. Seeburg, and B. Sakmann. 1992b. Control by asparagine residues of calcium permeability and magnesium blockade in the NMDA receptor. *Science.* 257:1415–1419.

Changeux, J. P., J. L. Galzi, A. Devillers-Thiéry, and D. Bertrand. 1992. The functional architecture of the acetylcholine nicotinic receptor explored by affinity labeling and site-directed mutagenesis. *Q. Rev. Biophys.* 25:395–432.

Deisenhofer, J., O. Epp, I. Sinning, and H. Michel. 1995. Crystallographic refinement at 2.3-angstrom resolution and model of the photosynthetic reaction center from *Rhodopseudomonas viridis*. *J. Mol. Biol.* 246: 429–457.

Dingledine, R., R. I. Hume, and S. F. Heinemann. 1992. Structural determinants of barium permeation and rectification in non-NMDA glutamate receptor channels. *J. Neurosci.* 12:4080–4087.

Durell, S. R., and H. R. Guy. 1992. Atomic scale structure and functional models of voltage-gated potassium channels. *Biophys. J.* 62:238–250.

Ealick, S. E., Y. S. Babu, C. E. Bugg, M. D. Erion, W. C. Guida, J. A. Montgomery, and J. A. Secrist, III. 1991. Application of crystallographic and modeling methods in the design of purine nucleoside phosphorylase inhibitors. *Proc. Natl. Acad. Sci. USA.* 88:11540–11544.

Egebjerg, J., B. Bettler, I. Hermans-Borgmeyer, and S. Heinemann. 1991. Cloning of a cDNA for a receptor subunit activated by kainate but not AMPA. *Nature.* 351:745–748.

Eisman, E., F. Muller, S. H. Heinemann, and U. B. Kaupp. 1994. A single negative charge within the pore region of a cGMP-gated channel controls rectification, Ca^{++} blockage, and ionic selectivity. *Proc. Natl. Acad. Sci. USA.* 91:1109–1113.

Evans, S. V. 1993. SETOR: hardware lighted three-dimensional solid model representations of macromolecules. *J. Mol. Graph.* 11:134–138.

Ferrer-Montiel, A. V., W. Sun, and M. Montal. 1995. Molecular design of the *N*-methyl-D-aspartate receptor binding site for phencyclidine and dizolcipine. *Proc. Natl. Acad. Sci. USA.* 92:8021–8025.

Geiger, J. R. P., T. Melcher, D.-S. Koh, B. Sakmann, P. H. Seeburg, P. Jonas, and H. Monyer. 1995. Relative Abundance of subunit mRNAs determines gating and Ca^{2+} permeability of AMPA receptors in principal neurons and interneurons in rat CNS. *Neuron.* 15:193–204.

Goulding, E. H., G. R. Tibbs, D. Liu, and S. A. Siegelbaum. 1993. Role of H5 domain in determining pore diameter and ion permeation through cyclic nucleotide-gated channels. *Nature.* 364:61–64.

Gregor, P., I. Mano, I. Maoz, M. McKeown, and V. Teichberg. 1989. Molecular structure of the chick cerebellar kainate-binding subunit of a putative glutamate receptor. *Nature.* 342:689–692.

Guy, H. R., and S. R. Durell. 1994. Using sequence homology to develop three-dimensional models of the transmembrane portions of potassium channels and homologous proteins. *J. Gen. Physiol.* 17:P7a. (Abstr.)

Heginbotham, L., T. Abramson, and R. MacKinnon. 1992. A functional connection between the pores of distantly related ion channels as revealed by mutant K^+ channels. *Science.* 258:1152–1155.

Henderson, R., J. M. Baldwin, T. A. Ceska, F. Zemlin, E. Beckmann, and K. H. Downing. 1990. Model for the structure of bacteriorhodopsin based on high-electron cryomicroscopy. *J. Mol. Biol.* 213:899–929.

Henley, J. M., and R. E. Oswald. 1988. Solubilization and characterization of kainate receptors from goldfish brain. *Biochim. Biophys. Acta.* 937: 102–111.

Higgins, D. G., A. J. Bleasby, and R. Fuchs. 1992. Clustal-V: improved software for multiple sequence alignment. *Computer Applications in the Biosciences.* 8:189–191.

Hille, B. 1984. Ionic Channels of Excitable Membranes. Sinauer Associates, Sunderland, MA.

Hollmann, M., and S. Heinemann. 1994. Cloned glutamate receptors. *Annu. Rev. Neurosci.* 17:31–108.

Hollmann, M., C. Maron, and S. Heinemann. 1994. *N*-Glycosylation site tagging suggests a three transmembrane domain topology for the glutamate receptor GluR1. *Neuron.* 13:1331–1343.

Hollmann, M., A. O'Shea-Greenfield, S. W. Rogers, and S. Heinemann. 1989. Cloning by functional expression of a member of the glutamate receptor family. *Nature.* 342:643–648.

Hume, R. I., R. Dingledine, and S. F. Heinemann. 1991. Identification of a site in glutamate receptor subunits that contols calcium permeability. *Science.* 253:1028–1031.

Imoto, K., C. Busch, B. Sakmann, M. Mishina, T. Konno, J. Nakai, H. Bujo, Y. Mori, K. Fukuda, and S. Numa. 1988. Rings of negatively charged amino acids determine the acetylcholine receptor channel conductance. *Nature.* 335:645–648.

Jones, D. T., W. R. Taylor, and J. M. Thornton. 1994. A model recognition approach to the prediction of all-helical membrane protein structure and topology. *Biochemistry.* 33:3038–3049.

Keinänen, K., W. Wisden, B. Sommer, P. Werner, A. Herb, T. A. Verdoorn, B. Sakmann, and P. H. Seeburg. 1990. A family of AMPA-selective glutamate receptors. *Science.* 249:556–560.

Köhler, M., N. Burnashev, B. Sakmann, and P. H. Seeburg. 1993. Determinants of Ca^{++} permeability in both TMI and TM2 of high affinity kainate receptor channels: diversity by RNA editing. *Neuron.* 10:491–500.

Kraulis, P. J. 1991. MolScript—a program to produce both detailed and schematic plots of protein structures. *J. Appl. Crystallogr.* 24:946–950.

Kuner, T., L. P. Wollmuth, P. H. Seeburg, and B. Sakmann. 1995. Probing the cytoplasmic face of the NMDA receptor channel port in cysteine-substitution mutants. *Soc. Neurosci. Abstr.* 21:85.

Kuntz, I. D., E. C. Meng, and B. K. Shiochet. 1994. Structure-based molecular design. *Acct. Chem. Res.* 27:117–123.

Kuryatov, A., B. Laube, H. Betz, and J. Kuhse. 1994. Mutational analysis of the glycine-binding site of the NMDA receptor: structural similarity with bacterial amino acid-binding proteins. *Neuron.* 12:1291–1300.

Kurz, L. L., R. D. Zuhlke, H. J. Zhang, and R. H. Joho. 1995. Side-chain accessibilities in the pore of a K+ channel probed by sulfhydryl-specific reagents after cysteine-scanning mutagenesis. *Biophys. J.* 68:900–905.

Li, F., N. Owens, and T. A. Verdoorn. 1995. Functional effects of mutations in the putative agonist binding region of recombinant α-amino-3-hydroxy-5-methyl-4-isoxazolepropionic acid receptors. *Mol. Pharmacol.* 47:148–154.

Liman, E. R., J. Tytgat, and P. Hess. 1992. Subunit stoichiometry of a mammalian K^+ channel determined by construction of multimeric cDNAs. *Neuron.* 9:861–871.

Lu, Q., and C. Miller. 1995. Silver as a probe of pore-forming residues in a potassium channel. *Science.* 268:304–307.

Mackerell, A. D., D. Bashford, M. Bellott, R. L. Dunbrack, H. S. Field, D. Joseph, L. Kuchnir, K. Kuczera, F. Lau, P. B. Mattos, B. Roux, M. Schlenkrich, J. Smith, R. Stote, and K. M. Straub. 1992. Self-consistent parameterization of biomolecules for molecular modeling and condensed phase simulations. *Biophys. J.* 61:A143.

MacKinnon, R. 1991. Determination of the subunit stoichiometry of a voltage-activated potassium channel. *Nature.* 350:232–235.

MacKinnon, R. 1995. Pore loops: an emerging theme in ion channel structure. *Neuron.* 14:889–892.

Merritt, E. A., and M. E. P. Murphy. 1994. Raster3D version 2.0: a program for photorealistic molecular graphics. *Acta Crystallogr.* D50: 869–873.

Monaghan, D. T., R. J. Bridges, and C. W. Cotman. 1989. The excitatory amino acid receptors: their classes, pharmacology, and distinct properties in the function of the central nervous system. *Annu. Rev. Pharmacol. Toxicol.* 29:365–402.

Nakanishi, N., N. A. Schneider, and R. Axel. 1990. A family of glutamate receptor genes: evidence for the formation of heteromultimeric receptors with distinct channel properties. *Neuron.* 5:569–581.

Nakanishi, S. 1992. Molecular diversity of glutamate receptors and implications for brain function. *Science.* 258:597–603.

Nakanishi, S., and M. Masu. 1994. Molecular diversity and functions of glutamate receptors. *Annu. Rev. Biophys. Biomol. Struct.* 23:319–348.

Nicholls, A., and B. Honig. 1991. A rapid finite difference algorithm using successive over-relaxation to solve the Poisson-Boltzmann equation. *J. Comp. Chem.* 12:435–445.

Oh, B. H., J. Pandit, C. H. Kang, K. Nikaido, S. Gokcen, G. F. L. Ames, and S. H. Kim. 1993. Three dimensional structure of the periplasmic lysine/arginine/ornithine-binding protein with and without a ligand. *J. Biol. Chem.* 268:11348–11355.

O'Hara, P. J., P. O. Sheppard, H. Thøgersen, D. Venezia, B. A. Haldeman, V. McGrane, K. M. Houamed, C. Thomsen, T. L. Gilbert, and E. R. Mulvihill. 1993. The ligand-binding domain in metabotropic glutamate receptors is related to bacterial periplasmic binding proteins. *Neuron.* 11:41–52.

Pascual, J. M., C. C. Shieh, G. E. Kirsch, and A. M. Brown. 1995. K^+ pore structure revealed by reported cysteines and inner and outer surfaces. *Neuron.* 14:1055–1063.

Person, B., and P. Argos. 1994. Prediction of transmembrane segments in proteins utilising multiple sequence alignments. *J. Mol. Biol.* 237: 182–192.

Roche, K. W., L. A. Raymond, C. Blackstone, and R. L. Huganir. 1994. Transmembrane topology of the glutamate receptor subunit GluR6. *J. Biol. Chem.* 269:11679–11682.

Root, M. J., and R. MacKinnon. 1993. Identification of an external divalent cation-binding site in the pore of a cGMP-activated channel. *Neuron.* 11:459–466.

Root, M. J., and R. MacKinnon. 1994. Two identical noninteracting sites in an ion channel revealed by proton transfer. *Science.* 265:1852–1856.

Rost, B., and C. Sander. 1994. Combining evolutionary information and neural networks to predict protein secondary structure. *Proteins.* 19: 55–72.

Sibanda, B. L., T. L. Blundell, and J. M. Thornton. 1989. Conformation of β-hairpins in protein structures. *J. Mol. Biol.* 206:759–777.

Sippl, M. J. 1993. Recognition of errors in three-dimensional structures of proteins. *Proteins.* 17:355–362.

Smart, O. S., J. M. Goodfellow, and B. A. Wallace. 1993. The pore dimensions of gramicidin A. *Biophys. J.* 65:2455–2460.

Sommer, B., K. Keinänen, T. A. Verdoorn, W. Wisden, N. Burnashev, A. Herb, M. Köhler, T. Takagi, G. Sakmann, and P. H. Seeburg. 1990. Flip and flop: a cell-specific functional switch in glutamate-operated channels of the CNS. *Science.* 249:1580–1584.

Sommer, B., M. Köhler, R. Sprengel, and P. H. Seeburg. 1991. RNA editing in brain controls a determinant of ion flow in glutamate-gated channels. *Cell.* 67:11–19.

Stanfield, P. R., N. W. Davies, P. A. Shelton, M. A. Sutcliffe, I. A. Khan, W. J. Brammar, and E. C. Conley. 1994. A single aspartate residue is involved in both intrinsic gating and blockage by Mg^{2+} of the inward rectifier, IRK1. *J. Physiol.* 478:1–6.

Stern-Bach, Y., B. Bettler, M. Hartley, P. O. Sheppard, P. J. O'Hara, and S. F. Heinemann. 1994. Agonist selectivity of glutamate receptors is specified by two domains structurally related to bacterial amino acid-binding proteins. *Neuron.* 13:1345–1357.

Sullivan, J. M., S. F. Traynelis, H. S. V. Chen, W. Escobar, S. F. Heinemann, and S. A. Lipton. 1994. Identification of two cysteine residues that are required for redox modulation of the NMDA subtype of glutamate receptor. *Neuron.* 13:929–936.

Surles, M. C., J. S. Richardson, D. C. Richardson, and F. P. J. Brooks. 1994. Sculpting proteins interactively: continual energy minimization embedded in a graphical modeling system. *Protein Sci.* 3:198–210.

Taverna, F. A., L. Y. Wang, J. F. MacDonald, and D. R. Hampson. 1994. A transmembrane model for an ionotropic glutamate receptor predicted

on the basis of the location of asparagine-linked oligosaccharides. *J. Biol. Chem.* 269:14159–14164.

Taylor, W. R. 1988. A flexible method to align large numbers of biological sequences. *J. Mol. Evol.* 28:161–169.

Uchino, S., K. Sakimura, K. Nagahari, and M. Mishina. 1992. Mutations in a putative agonist binding region of the AMPA-selective glutamate receptor channel. *FEBS Lett.* 308:253–257.

Verdoorn, T. A., N. Burnashev, H. Monyer, P. H. Seeburg, and B. Sakmann. 1991. Structural determinants of ion flow through recombinant glutamate receptor channels. *Science.* 252:1715–1718.

Villarroel, A., N. Burnashev, and B. Sakmann. 1995. Dimensions of the narrow portion of a recombinant NMDA receptor channel. *Biophys. J.* 68:866–875.

Wada, K., C. J. Dechesne, S. Shimasaki, R. G. King, K. Kusano, A. Buonanno, D. R. Hampson, C. Banner, R. J. Wenthold, and Y. Nakatani. 1989. Sequence and expression of a frog brain complementary DNA encoding a kainate-binding protein. *Nature.* 342:684–689.

Weiner, S. J., P. A. Kollmann, D. A. Case, U. C. Singh, C. Ghio, G. Alagona, S. J. Profeta, and P. Weiner. 1984. A new forcefield for molecular mechanical simulations of nucleic acids and proteins. *J. Am. Chem. Soc.* 106:765–784.

Wenthold, R. J., N. Yokotani, K. Doi, and K. Wada. 1992. Immunochemical characterization of the non-NMDA glutamate receptor using subunit-specific antibodies. *J. Biol. Chem.* 267:501–507.

Wisden, W., and P. Seeburg. 1993. Mammalian ionotropic glutamate receptors. *Curr. Opin. Neurobiol.* 3:291–298.

Wo, Z. G., and R. E. Oswald. 1994. Transmembrane topology of two kainate receptor subunits revealed by N-glycosylation. *Proc. Natl. Acad. Sci. USA.* 91:7154–7158.

Wo, Z. G., and R. E. Oswald. 1995a. Asn265 of frog kainate binding protein is a functional glycosylation site: implications for the transmembrane topology of glutamate receptors. *FEBS Lett.* 368:230–234.

Wo, Z. G., and R. E. Oswald. 1995b. A topological analysis of goldfish kainate receptors predicts three transmembrane segments. *J. Biol. Chem.* 270:2000–2009.

Wo, Z. G., and R. E. Oswald. 1995c. Unraveling the modular design of glutamate-gated ion channels. *Trends Neurosci.* 18:161–168.

Wood, M. W., H. M. A. VanDongen, and A. M. J. VanDongen. 1995. Structural conservation of ion conduction pathways in K channels and glutamate receptors. *Proc. Natl. Acad. Sci. USA.* 92:4882–4886.

Woodhull, A. M. 1973. Ionic blockade of sodium channels in nerve. *J. Gen. Physiol.* 61:687–708.

Wu, T. Y., and Y. C. Chang. 1994. Hydrodynamic and pharmacological characterization of putative alpha-amino-3-hydroxy-5-methyl-4-isoxazolepropionic acid kainate-sensitive L-glutamate receptors solubilized from pig brain. *Biochem. J.* 300:365–371.

Yao, N. H., S. Trakhanov, and F. A. Quicho. 1994. Refined 1.89 Å structure of the histidine-binding protein complexed with histidine and its relationship with many other active transport/chemosensory proteins. *Biochemistry.* 33:4769–4779.

Zarei, M. M., and J. A. Dani. 1995. Structural basis for explaining open-channel blockade of the NMDA receptor. *J. Neurosci.* 15:1446–1454.